

# Microsecond Motions of the Lipids Associated with Trypsinized Na,K-ATPase Membranes. Progressive Saturation Spin-Label Electron Spin Resonance Studies<sup>†</sup>

Ashish Arora,<sup>‡,§</sup> Mikael Esmann,<sup>||</sup> and Derek Marsh<sup>\*,‡</sup>

Max-Planck-Institut für biophysikalische Chemie, Abteilung Spektroskopie, D-37070 Göttingen, Germany, and  
Department of Biophysics, University of Aarhus, DK-8000 Aarhus C, Denmark

Received November 11, 1998; Revised Manuscript Received May 24, 1999

**ABSTRACT:** The microsecond motions of spin-labeled lipids associated with the Na<sup>+</sup>/K<sup>+</sup>-transporting ATP hydrolase (Na,K-ATPase) in native and tryptically shaved membranes from *Squalus acanthias* have been studied by progressive saturation electron spin resonance (ESR). This includes both the segmental mobility of the lipid chains and the exchange dynamics of the lipids interacting directly with the protein. The lipids at the protein interface display a temperature-dependent chain mobility on the submicrosecond time scale. Exchange of these lipids with those in the bulk bilayer regions of the membrane takes place on the time scale of the nitroxide spin–lattice relaxation, i.e., in the microsecond regime. The off-rates for exchange directly reflect the specificity of ionized fatty acids relative to protonated fatty acids for interaction with the Na,K-ATPase. These essential features of the lipid dynamics at the intramembranous protein surface, namely, a temperature-dependent exchange on the microsecond time scale that reflects the lipid selectivity, are preserved on removing the extramembranous parts of the Na,K-ATPase by extensive trypsinization.

The intramembranous section of the Na,K-ATPase<sup>1</sup> ion pump interacts with a first shell of lipids, the composition and chain mobility of which differs from that of the surrounding bulk lipids (1). The exact transmembrane topology of the Na,K-ATPase  $\alpha$ -subunit is not known with certainty, but, in principle, the nature of the lipid–protein interactions can shed some light on this (e.g., refs 2 and 3). Advances in understanding the arrangement of the intramembranous sections of the protein have come from extensive trypsinolysis of both the kidney (4) and shark enzymes (5, 6). For the latter, proteolysis by this protocol yields membranous preparations that either retain or are devoid of the capacity to occlude Rb<sup>+</sup>, depending on whether trypsinization is performed in the presence of Rb<sup>+</sup> or of Na<sup>+</sup>, respectively. Rb occlusion capacity appears to be associated with the intactness of a C-terminal 19 kDa fragment that has four putative transmembrane segments (4). In models with 10 transmembrane segments of the  $\alpha$ -subunit and a single transmembrane segment of the 35 kDa glycosylated  $\beta$ -subunit (see, e.g., ref 7), a close interaction between segments M7–M10 (the 19 kDa fragment) and the  $\beta$  subunit has been proposed (8, 9). In addition, two of the minor tryptic

peptides of the  $\alpha$ -subunit (M1–M2 and M5–M6) interact with the 19 kDa fragment (10, 11). It appears that the transmembrane segments form a closely knit cluster of peptides, presumably with no intercalated lipid. Recent evidence also points to a certain plasticity of the complex of tryptic fragments, for example leading to a temperature-dependent release of the M5–M6 peptide from the membranes (12, 13).

Previously, we have compared the overall lipid–protein interactions of control and trypsinized Na,K-ATPase membranes, and found the major features, namely, stoichiometry and selectivity, to be similar (6, 14). In the present work, we look at the dynamics of the lipid–protein interactions by using spin label ESR saturation methods that are sensitive to lipid motions on the microsecond time scale (see ref 15 for a review). This includes both in situ motions of the protein-associated lipids and their exchange with the bulk pool of lipids in the membrane (16, 17). Previous studies with the myelin proteolipid protein have shown that lipid exchange rates at the protein interface are comparable with the spin–lattice relaxation rate of the spin label or are slower, depending on the mobility state of the host lipid (17, 18). They also directly reflect the thermodynamic selectivity of lipid interaction with the protein (19). Such dynamic features as these give a more detailed characterization of the lipid–protein interface and its possible modification on trypsinization of the Na,K-ATPase protein. Preservation of the lipid–protein interactions of the intact system is essential if the trypsinized Na,K-ATPase preparations are to yield reliable information on assembly of the intramembranous section of this active transport enzyme.

<sup>†</sup> This work was supported in part by the Human Frontiers Science Program (RG-511/95).

<sup>‡</sup> Max-Planck-Institut für biophysikalische Chemie.

<sup>§</sup> Present address: Department of Molecular Physiology & Biological Physics, University of Virginia, Health Sciences Center, Charlottesville, VA 22906-0011.

<sup>||</sup> University of Aarhus.

<sup>1</sup> Abbreviations: Na,K-ATPase, Na<sup>+</sup>/K<sup>+</sup>-transporting ATP hydrolase (EC 3.6.1.37); ESR, electron spin resonance; 14-SASL, 14-(4,4-dimethylloxazolidine-*N*-oxyl)stearic acid; p–p, peak-to-peak; tris, tris(hydroxymethyl)aminomethane; CDTA, *trans*-1,2-cyclohexylenedinitrotetraacetic acid; EDTA, ethylenediaminetetraacetic acid; SDS, sodium dodecyl sulfate.

## MATERIALS AND METHODS

**Preparation of Shark Rectal Gland Na,K-ATPase.** Na,K-ATPase from the rectal gland of *S. acanthias* was prepared as described previously (20) but omitting the treatment with saponin. The Na,K-ATPase constituted typically 70% of the total protein (determined as the content of  $\alpha$ - and  $\beta$ -subunits from SDS gel electrophoresis), and the specific activity was 1400–1700  $\mu\text{mol}$  of ATP hydrolyzed  $(\text{mg of protein})^{-1} \text{h}^{-1}$ . Na,K-ATPase activity and protein content were determined as previously described (21). Membrane lipids were extracted with  $\text{CHCl}_3/\text{CH}_3\text{OH}$  (2:1 v/v) (22).

**Trypsinization of Na,K-ATPase.** Na,K-ATPase membranes were incubated at a concentration of 0.9 mg/mL with 10 mM RbCl or NaCl, 15 mM histidine, and 1 mM CDTA (pH 7.0 at 20 °C) with trypsin (final concentration 0.5 mg/mL). After 60 min at 23 °C, a 10-fold excess by weight of trypsin inhibitor was added, in the same buffer, and the sample was allowed to stand for 10 min at 23 °C. The membranes were washed by centrifugation three times in a buffer containing 10 mM RbCl or NaCl, 15 mM histidine, 1 mM CDTA (pH 7.0 at 20 °C), and 25% glycerol (23). Samples were stored at –20 °C in this buffer. Control enzyme was treated as above but trypsin was omitted. Trypsin (T-8642), trypsin inhibitor (T-9128), histidine, and Tris were obtained from Sigma Chemical Co. (St. Louis, MO). All other reagents were of the highest purity available.

**ESR Sample Preparation.** Stearic acid (14-SASL) spin-labeled on the 14-C atom of the chain was prepared as described in ref 24. Membranous Na,K-ATPase (native, control, or trypsinized) protein (2 mg) was incubated at 23 °C for 15 min, either in 10 mL of histidine buffer (10 mM, pH 6.0) with 40  $\mu\text{g}$  of spin-labeled lipid or in 10 mL of Tris buffer (10 mM, with 1 mM EDTA, pH 9.0) with 80  $\mu\text{g}$  of spin-labeled lipid, added as a concentrated ethanol solution (10 mg/mL). Membranes were pelleted by centrifugation at 45 000 rpm for 45 min at 4 °C. The pellet was taken up into a 1-mm diameter glass capillary and trimmed to a sample length of 5 mm. Lipid dispersions were labeled by codissolving the spin label with extracted membrane lipids in  $\text{CHCl}_3/\text{CH}_3\text{OH}$  (2:1 v/v), prior to removal of the organic solvent, drying, and subsequent dispersion of the lipid in buffer.

Samples were prepared as matched series of the different membrane preparations at the different pH values, to obtain as far as possible identical labeling and measuring conditions. Means of duplicate or triplicate series are reported. In Table 2, values are derived by combining measurements at two pH values; therefore in this case the error limits for a given membrane type are strictly correlated.

**ESR Spectroscopy.** ESR spectra were recorded on a Varian Century Line 9 GHz spectrometer equipped with nitrogen gas flow temperature regulation. The glass capillaries were placed in a standard quartz holder (4 mm i.d.) containing light silicone oil for thermal stability. Spectral data were collected digitally on an IBM personal computer using software written by M. D. King of this institute. Spectral subtractions were performed as described earlier (25). Conventional, in-phase, absorption spectra ( $V_1$  display) were recorded, with a scan range of 160 G and a modulation amplitude of 1.0 G p-p, at various microwave powers decreasing from 200 to 0.2 mW, which corresponds to a root-

mean-square (rms) microwave magnetic field,  $\langle H_1^2 \rangle^{1/2}$ , of 600–6 mG at the sample. A standardized sample configuration was used in all progressive saturation experiments (26), and all measurements were performed under critical coupling conditions. Corrections for changes in cavity  $Q$ -factor between different samples were performed as described in ref 26. The saturation curves were obtained by plotting the spectral intensity (second integral of the first derivative spin-label ESR spectrum) as a function of the rms microwave magnetic field,  $\langle H_1^2 \rangle^{1/2}$ , at the sample and were analyzed as described in refs 27 and 28. The  $H_1$  dependence of the double-integrated intensity,  $S$ , of the spin label ESR spectrum is given by (28)

$$S = \frac{S'_0 H_1}{\{1 + \gamma_e^2 \langle H_1^2 \rangle (T_1 T_2)^{\text{eff}}\}^{1/2}} \quad (1)$$

where  $\gamma_e$  is the electron gyromagnetic ratio,  $(T_1 T_2)^{\text{eff}}$  is the effective  $T_1 T_2$  relaxation time product, and  $S'_0$  is a normalization constant. Spectral double integrals were evaluated over the full scan range of 160 G. Peak-to-peak line widths of the central hyperfine line were determined by local fitting to the spectral peaks.

## RESULTS

Progressive saturation of the ESR spectrum with increasing microwave power was used to study the chain motions of a spin-labeled fatty acid that take place on the time scale,  $T_1$ , of the spin–lattice relaxation, which is typically in the microsecond regime (15). Comparison of results from spin-labeled lipids in Na,K-ATPase membranes and in dispersions of the extracted membrane lipids is used to give information on the motional restriction of the lipids directly associated with the Na,K-ATPase and on their exchange with the bulk membrane lipids. Measurements are made on the protonated fatty acid (at pH 6.0), and on the negatively charged form (at pH 9.0) that exhibits a higher selectivity for interaction with the Na,K-ATPase (29). Combination of the data at both pH values is needed to estimate the exchange rates, because the saturation behavior of the protein-associated lipids in isolation is not directly accessible. Measurements at low and relatively high temperatures are used to further characterize the lipid dynamics. Comparisons are made between control membranes and those that have been extensively trypsinized in the presence of either  $\text{Na}^+$  or  $\text{Rb}^+$  ions, to assess to what extent, if any, the dynamics of the lipid chains at the intramembranous surface of the protein are modified on trypsinization.

**Measurements at 4 °C.** Figure 1 gives the ESR spectra of the 14-SASL stearic acid spin label at pH 9.0 in control Na,K-ATPase membranes and in dispersions of the extracted membrane lipids, at 4 °C. The spectra were recorded at increasing values of the microwave power, as indicated on the figure. The nonsaturated membrane spectra (solid line), at low power (e.g.,  $\langle H_1^2 \rangle^{1/2} = 0.057 \text{ G}$ ), are two-component in nature. One component closely resembles the spectrum from dispersions of the extracted membrane lipids (dashed line). The other component has much larger spectral splittings and corresponds to the spin-labeled lipid population that is interacting directly with the intramembranous surface of the Na,K-ATPase protein (29). At pH 9.0 this latter component

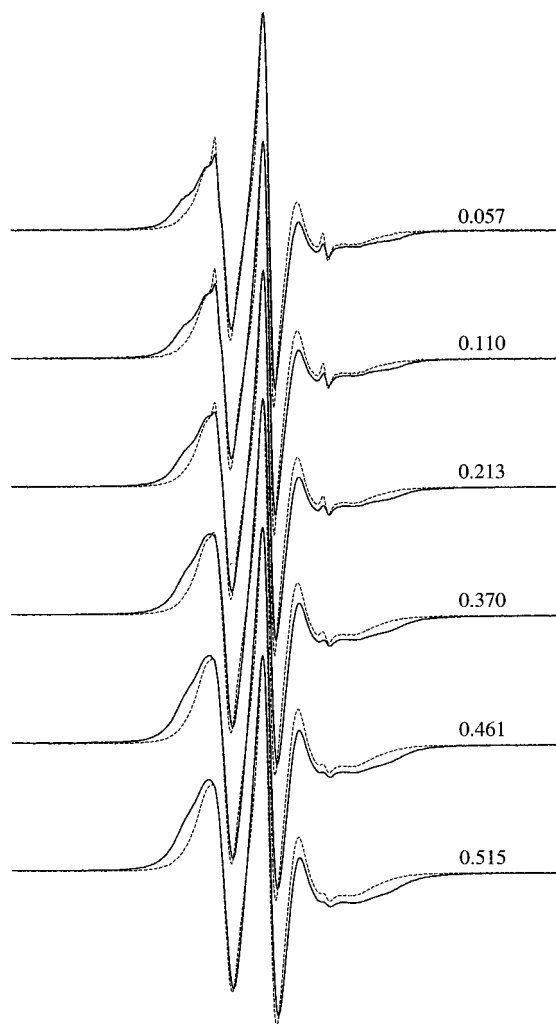


FIGURE 1: ESR spectra of the 14-SASL stearic acid spin label in control Na,K-ATPase membranes (solid lines) and in dispersions of the extracted Na,K-ATPase membrane lipids (dashed lines) at pH 9.0 and 4 °C, recorded at the microwave  $H_1$  field intensities,  $\langle H_1^2 \rangle^{1/2}$  (in gauss), indicated on the figure. Total scan width = 160 G.

has a high relative intensity and dominates the two-component membrane spectra, because of the strong relative selectivity of the negatively charged form of stearic acid for the Na,K-ATPase (14). The fraction,  $f$ , of this motionally restricted protein-interacting component can be obtained by spectral subtraction (using the extracted lipid spectra) and integration as described previously (30). These values are given in Table 1.

The ESR spectra in Figure 1 are normalized to the same maximum line height. Therefore, they reflect the saturation broadening of the spectral line shapes with increasing microwave power but not the effect of saturation on the spectral intensities. The saturation curves for the double-integrated intensities of the first harmonic spectra (cf. ref 28) are given in Figure 2 for 14-SASL at pH 9.0 in control membranes, membranes trypsinized in  $Rb^+$  or in  $Na^+$ , and in dispersions of the extracted membrane lipids, each at 4 °C. All saturation curves have the same vertical normalization in Figure 2, which can be seen from the fact that all have the same linear dependence on  $H_1$  in the nonsaturating region at low powers. The different membranous samples saturate differently, however, at high microwave powers. In particular,

the lipid sample saturates less readily than do the membrane samples. The saturation curves for the membrane samples, in addition to those for the extracted lipids, are fitted well by eq 1, which describes the saturation behavior for the integrated intensities of a single spectral component (see Figure 2). It was shown previously that this is the case for two-component spectra, such as the membrane samples, if the effective  $T_1T_2$  relaxation time products of the two components differ by less than a factor of 10 (28). This is therefore the case for 14-SASL in both the control and trypsinized Na,K-ATPase membrane samples studied here. The effective values of the  $T_1T_2$  relaxation time products that are obtained from the fits given in Figure 2 are listed in Table 1 for control, trypsinized, and extracted lipid samples, as well as for native membranes that have not undergone the incubation procedure that is involved in the trypsinization protocol (see Materials and Methods).

The data are tabulated as the effective relaxation rates for the various membrane samples,  $1/(T_1T_2)_M$ , and for dispersions of the extracted membrane lipids,  $1/(T_1T_2)_L$ , at 4 °C. The effective relaxation rates are lower for the membrane samples than for the lipid dispersions, in all cases. This corresponds to the motional restriction of the spin-labeled lipids that are in contact with the intramembranous section of the protein in the two-component membrane systems and is characterized by the intrinsic relaxation rate,  $1/(T_1T_2)_b^0$ , in this environment. It should be noted that this difference between lipids in bilayers and at the protein interface (and the corresponding difference between the intrinsic relaxation parameters at 25 °C given later) establishes an internally consistent comparative scale for the dependence of the relaxation rates on the dynamics of the environment. (A theoretical calibration for the sensitivity to rotational dynamics is given later in Figure 4.) The effective relaxation rates for membranes at pH 9.0 are lower than those for membranes at pH 6.0, in each system. At least in part, this is because of the higher fraction,  $f$ , of ionized stearic acid that is associated with the protein at pH 9.0 than that of the protonated stearic acid at pH 6.0 (cf. refs 14 and 29).

The saturation behavior of the integrated intensity for the two-component ESR spectra from the membrane systems is given by

$$S = S_0 \left[ \frac{f}{\{1 + \sigma_M(T_1T_2)_b/(T_1T_2)_M\}^{1/2}} + \frac{1-f}{\{1 + \sigma_M(T_1T_2)_f/(T_1T_2)_M\}^{1/2}} \right] \quad (2)$$

where  $S_0$  is the value that  $S$  would have in the absence of saturation,  $(T_1T_2)_M$  is the effective relaxation time product obtained from eq 1 for the two-component membrane system, and  $\sigma_M = \gamma_e^2 \langle H_1^2 \rangle (T_1T_2)_M$  is the corresponding saturation factor. The effective relaxation time products for the protein-associated and fluid bilayer lipids are given by  $(T_1T_2)_b$  and  $(T_1T_2)_f$ , respectively. In the absence of exchange between the two spin-labeled lipid populations, these relaxation time products will have the values intrinsic to the single populations, i.e.,  $(T_1T_2)_b^0$  and  $(T_1T_2)_f^0$ , respectively, where the latter is equal to the value,  $(T_1T_2)_L$ , measured in dispersions of the extracted membrane lipids.

At a temperature of 4 °C, it might be expected that the exchange rate between the two lipid populations will be slow

Table 1: Relaxation Rates for 14-SASL Stearic Acid Spin Label at 4 °C<sup>a</sup>

membrane	pH	<i>f</i>	$1/(T_1T_2)_M$ ( $\times 10^{-13} \text{ s}^{-2}$ )	$1/(T_1T_2)_L$ ( $\times 10^{-13} \text{ s}^{-2}$ )	$1/(T_1T_2)_b^0$ ( $\times 10^{-13} \text{ s}^{-2}$ )
native <sup>b</sup>	6.0	0.250 ± 0.002	12.6 ± 0.1	13.7 ± 0.6	10.0 ± 1.7
	9.0	0.464 ± 0.004	9.6 ± 0.04	13.7 ± 0.6	6.3 ± 0.4
control <sup>b</sup>	6.0	0.260 ± 0.002	10.6 ± 0.3	13.7 ± 0.6	4.9 ± 1.3
	9.0	0.452 ± 0.004	8.8 ± 0.3	13.7 ± 0.6	5.0 ± 0.7
Rb-trypsin	6.0	0.262 ± 0.002	9.0 ± 0.3	13.7 ± 0.6	2.3 ± 0.9
	9.0	0.392 ± 0.002	7.9 ± 0.04	13.7 ± 0.6	3.0 ± 0.3
Na-trypsin	6.0	0.262 ± 0.001	10.4 ± 0.15	13.7 ± 0.6	4.5 ± 1.0
	9.0	0.400 ± 0.003	8.4 ± 0.3	13.7 ± 0.6	3.8 ± 0.7

<sup>a</sup> Experimental rates are given for 14-SASL in Na,K-ATPase membranes,  $1/(T_1T_2)_M$ , and in dispersions of extracted membrane lipids,  $1/(T_1T_2)_L$ , together with values,  $1/(T_1T_2)_b^0$ , predicted for the protein-associated spin-labeled lipids assuming no exchange according to eq 2. *f* is the fraction of protein-associated spin-labeled lipid. <sup>b</sup> Values of relaxation parameters for native and control membranes differ because of changes in protein dynamics that occur in the control sample during incubation in the absence of trypsin (31); see text.

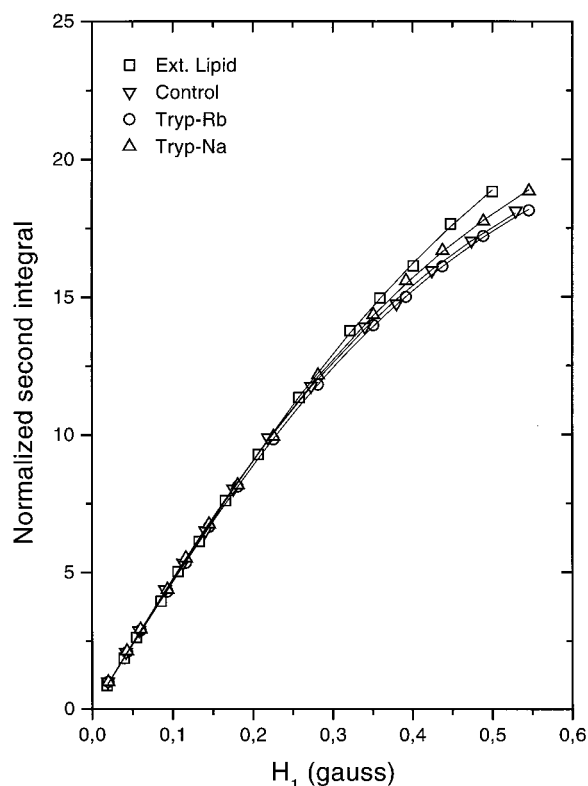


FIGURE 2: Saturation curves, as a function of  $H_1$  field strength, for the double-integrated intensity of the ESR spectra of 14-SASL stearic acid spin label in control Na,K-ATPase membranes ( $\nabla$ ), Rb-trypsinized Na,K-ATPase membranes ( $\circ$ ), Na-trypsinized Na,K-ATPase membranes ( $\Delta$ ), and dispersions of extracted Na,K-ATPase membrane lipids ( $\square$ ), at pH 9.0 and 4 °C. Continuous lines represent nonlinear least-squares fitting to eq 1.

on the spin label  $T_1$  time scale.<sup>2</sup> The effective relaxation products for the protein-associated spin-labeled component,  $(T_1T_2)_b^0$ , obtained from eq 2 by neglecting exchange between the lipid populations, are given in Table 1. For this determination, eq 2 was evaluated with  $\sigma_M = 3$ , i.e., for the condition of half-saturation:  $S_0/S = 1/2$ . It is seen from Table 1 that for each membrane system, with the exception of the native membranes, comparable values are obtained for the intrinsic relaxation rate of the protein-associated spin labels at both pH values, despite the different fractional populations. This result might be expected because the spin label group is in a similar location at the intramembraneous lipid-protein interface in each case. (Any possible difference in location

must, in any case, have a much smaller effect on the saturation parameters than does the difference between environments at the lipid/protein interface and bilayer regions of the membrane.) Also, the line shapes of the protein-associated lipid spin-label component obtained by spectral subtraction are very similar at both pH values (29). The consistency of the values of  $(T_1T_2)_b^0$  at different pH therefore supports the expectation that lipid exchange is not making an appreciable contribution to the effective relaxation rates at 4 °C. The exception to this is the native membrane, where it is possible that there may be a measurable contribution to the relaxation properties from lipid exchange, even at 4 °C. The relaxation properties in the presence of exchange are considered below, in connection with the measurements at higher temperature.

*Measurements at 25 °C.* Figure 3 gives the ESR spectra of the 14-SASL stearic acid spin label at pH 9.0 in control Na,K-ATPase membranes (solid lines) and in dispersions of the extracted membrane lipids (dashed lines) at 25 °C. The motionally restricted lipid spectral component is still visible in the outer wings of the membrane spectra at this temperature. The spectral component from the fluid lipids, in both membranes and lipid dispersions, however, has undergone considerable motional narrowing because of the increased rotational mobility of the lipid chains at this higher temperature (cf. Figure 1). In consequence, the exchange of spin-labeled lipids between the protein-associated and fluid bilayer environments will be faster at this higher temperature.

The method for analyzing the saturation behavior of the spin-label spectra that was used in Figure 2 has been shown by spectral simulations to be valid also in the presence of rotational motional averaging (33). The resulting values of the effective  $T_1T_2$  relaxation time products derived in this

<sup>2</sup> From previous results on the dynamics in Na,K-ATPase membranes, the exchange rate at 4 °C is expected to be much slower (relative to  $T_1$ ) than at 25 °C. Both the rotational diffusion (31) and translational diffusion (32) rates of the protein, which directly reflect the lipid mobility, are much slower at 4 °C than at 25 °C. Also, the angular amplitude of the spin-labeled lipid chain motion is much more restricted at 4 °C than at 25 °C (see ref 1, and compare Figures 1 and 3). In membranes containing the myelin proteolipid protein, the lipid exchange rates in the fluid phase at 30 °C are on the time scale of spin-label  $T_1$  relaxation, whereas in the gel phase at 4 °C they are immeasurably slow on this time scale (17). It therefore is expected that in the Na,K-ATPase membranes the exchange rates will be slow relative to the  $T_1$  time scale at 4 °C, although the membranes are not actually in a gel phase.

way from the microwave power dependence of the ESR spectra at 25 °C are given in Table 2.

The values of the effective relaxation rates,  $1/(T_1T_2)_M$  and  $1/(T_1T_2)_L$ , at 25 °C are higher than those obtained at 4 °C for all systems, particularly for the membrane samples (cf. Table 1). The higher rates at 25 °C can be attributed to exchange between the lipid populations and also to changes in the intrinsic relaxation rates of the two populations (15, 17). Again, for the membranes, the rates are lower at pH 9.0 than at pH 6.0, as would be expected from the different sizes of the motionally restricted lipid populations.

In the presence of exchange, the effective spin–lattice relaxation rates of the two lipid spin-label populations are modified from their intrinsic values according to (17)

$$\frac{T_{1,b}^0}{T_{1,b}} = 1 + \left(\frac{1-f}{f}\right) \frac{T_{1,b}^0 \tau_f^{-1}}{1 + T_{1,f}^0 \tau_f^{-1}} \quad (3)$$

$$\frac{T_{1,f}^0}{T_{1,f}} = 1 + \frac{T_{1,f}^0 \tau_f^{-1}}{1 + (1/f - 1)T_{1,b}^0 \tau_f^{-1}} \quad (4)$$

where  $T_{1,f}^0$ ,  $T_{1,b}^0$  are the intrinsic spin–lattice relaxation times of the fluid and protein-associated spin-labeled lipid populations, in the absence of exchange. Because the exchange is slow enough that it affects only  $T_1$  and not  $T_2$ , eqs 3 and 4 also give the ratio of the effective relaxation products, i.e.,  $(T_1T_2)_b^0/(T_1T_2)_b$  and  $(T_1T_2)_f^0/(T_1T_2)_f$ , respectively.<sup>3</sup> The intrinsic exchange off-rate for the protein-associated lipids,  $\tau_b^{-1}$ , is related to the on-rate,  $\tau_f^{-1}$ , for the fluid lipids, that is given in eqs 3 and 4 by the material balance condition for one-to-one lipid exchange:

$$f\tau_b^{-1} = (1-f)\tau_f^{-1} \quad (5)$$

The on-rate,  $\tau_f^{-1}$ , is found to be constant for a given lipid/protein ratio, i.e., is diffusion-controlled, whereas the off-rate,  $\tau_b^{-1}$ , reflects the intrinsic selectivity of interaction of the spin-labeled lipid with the protein (19, 34). The values in eqs 3 and 4 can be expressed in terms of a single normalized exchange rate  $T_{1,f}^0\tau_b^{-1}$ , together with the ratio  $(T_{1,f}^0/T_{1,b}^0)$ . The latter is obtained from the progressive saturation parameters, together with line width measurements:  $(T_{1,f}^0/T_{1,b}^0) = (T_1T_2)_b^0/(T_1T_2)_b^0 W_f^0/W_b^0$ , where  $W_f^0$  is the peak-to-peak line width from the lipid dispersion and  $W_b^0$  is determined from the membrane sample at pH 9.0, the line shape of which is dominated by the protein-associated spin label component. The two unknown quantities in eqs 3 and 4 are then only the intrinsic relaxation parameters of the protein-associated lipid component and the normalized exchange rate. To obtain an absolute exchange rate from the normalized value requires an independent

<sup>3</sup> The spin label  $T_2$  is much shorter than  $T_1$ , i.e., it is in the nanosecond regime as opposed to the microsecond regime, in Na,K-ATPase membranes. Therefore, lipid exchange rates that are in the megahertz (i.e., microsecond<sup>-1</sup>) range make a negligible contribution fractionally to the  $T_2$  relaxation rates but a proportionally larger one to the  $T_1$  relaxation rates. The ESR spectra from Na,K-ATPase membranes are intrinsically rather broad, because of relatively low lipid mobility and high cholesterol content. Consequently, lipid exchange makes a negligible contribution to the line widths, i.e., to  $T_2$  relaxation rates, in the present studies (cf. ref 19).

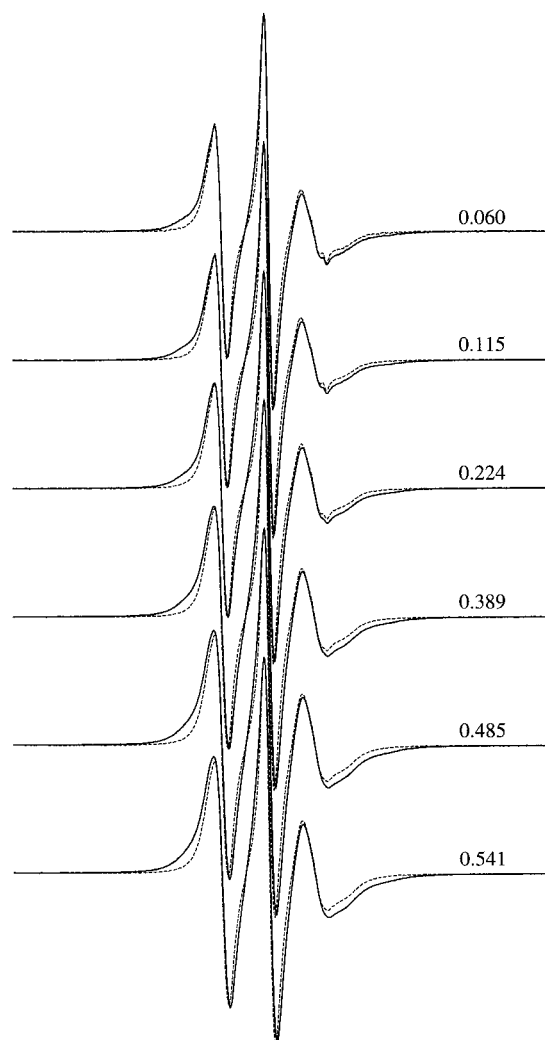


FIGURE 3: ESR spectra of the 14-SASL stearic acid spin label in control Na,K-ATPase membranes (solid lines) and in dispersions of the extracted Na,K-ATPase membrane lipids (dashed lines) at pH 9.0 and 25 °C, recorded at the microwave  $H_1$  field intensities,  $\langle H_1^2 \rangle^{1/2}$  (in gauss), indicated on the figure. Total scan width = 160 G.

determination of the spin–lattice relaxation time,  $T_{1,f}^0$ , in the lipid dispersion (see Discussion section).

For each membrane sample at 25 °C, the measurements at pH 6.0 and 9.0 have been combined, by assuming that the intrinsic relaxation parameters of the protein-associated spin label are the same at the two pH values, as reasoned above to be approximately the case at 4 °C. (This approach is valid irrespective of whether the spin label has the same location at both pH values or simply the intrinsic relaxation parameters are insensitive to slightly different locations at the lipid–protein interface.) The on-rate is the same at both pH values, because it is diffusion-controlled and the lipid/protein ratio is unchanged (see above and ref 34). Therefore, values for the exchange rate and the intrinsic relaxation parameters of the protein-associated spin label can be obtained from the measurements at the two pH values, by use of eqs 2–5. These results are given in the last two columns of Table 2, where again the condition corresponding to half-saturation ( $\sigma_M = 3$ ) is used for the evaluation. The exchange rates are normalized to the intrinsic  $T_1$  relaxation time of the fluid lipid component,  $T_{1,f}^0$ , because this component is common to all systems. The apparent exchange

Table 2: Relaxation Rates for 14-SASL Stearic Acid Spin Label at 25 °C<sup>a</sup>

membrane	pH	f	$1/(T_1T_2)_M$ ( $\times 10^{-13} \text{ s}^{-2}$ )	$1/(T_1T_2)_L$ ( $\times 10^{-13} \text{ s}^{-2}$ )	$1/(T_1T_2)_b^0$ ( $\times 10^{-13} \text{ s}^{-2}$ )	$T_{1,f}^0\tau_b^{-1}$
native	6.0	0.250 ± 0.002	17.0 ± 1.0	14.0 ± 0.7	5.2 <sup>-1.5</sup> <sub>-1.3</sub>	2.1 <sup>+4.7</sup> <sub>-1.3</sub>
	9.0	0.464 ± 0.004	14.5 ± 1.2	14.0 ± 0.7	5.2 <sup>+1.8</sup> <sub>+1.8</sub>	0.8 <sup>+1.3</sup> <sub>-0.5</sub>
control	6.0	0.260 ± 0.002	14.9 ± 0.1	14.0 ± 0.7	5.5 <sup>-1.4</sup> <sub>+0.4</sub>	0.7 <sup>+0.5</sup> <sub>-0.3</sub>
	9.0	0.452 ± 0.004	12.5 ± 0.1	14.0 ± 0.7	5.5 <sup>+1.4</sup> <sub>+0.4</sub>	0.3 <sup>+0.2</sup> <sub>-0.1</sub>
Rb-trypsin	6.0	0.262 ± 0.002	12.8 ± 1.9	14.0 ± 0.7	3.4 <sup>b</sup>	0.4 <sup>b</sup>
	9.0	0.392 ± 0.002	10.7 ± 0.7	14.0 ± 0.7	3.4 <sup>b</sup>	0.2 <sup>b</sup>
Na-trypsin	6.0	0.262 ± 0.001	14.2 ± 0.3	14.0 ± 0.7	7.4 <sup>-2.2</sup> <sub>+2.3</sub>	0.4 <sup>+0.6</sup> <sub>+0.3</sub>
	9.0	0.400 ± 0.003	12.9 ± 0.3	14.0 ± 0.7	7.4 <sup>+2.3</sup> <sub>+2.8</sub>	0.2 <sup>+0.3</sup> <sub>-0.2</sub>

<sup>a</sup> Experimental rates are given for 14-SASL in Na,K-ATPase membranes,  $1/(T_1T_2)_M$ , and in dispersions of extracted membrane lipids,  $1/(T_1T_2)_L$ , together with values,  $1/(T_1T_2)_b^0$ , predicted for the protein-associated spin-labeled lipids, assuming these to be equal at pH 6.0 and pH 9.0, and their normalized exchange rates,  $T_{1,f}^0\tau_b^{-1}$ , that are obtained from eqs 2–5. *f* is the fraction of protein-associated spin-labeled lipid. Taking a value of  $T_{1,f}^0 = 0.44 \mu\text{s}$  (see Discussion section), the absolute values of the exchange off-rate are  $\tau_b^{-1} = 4.1, 1.6, 1.6, 0.7, 0.9, 0.5, 0.7,$  and  $0.5 \times 10^6 \text{ s}^{-1}$ , corresponding to the values given from top to bottom in the last column. Derived errors in the values  $1/(T_1T_2)_b^0$  and  $T_{1,f}^0\tau_b^{-1}$  for the various samples are strictly correlated according to suffix position (upper or lower). <sup>b</sup> At extreme error limits, numerical solution does not converge.

rates are of a similar order of magnitude to those obtained for spin-labeled stearic acid interacting with the myelin proteolipid protein at pH 7.4 in a fluid phosphatidylcholine membrane, in the absence of cholesterol (17). When the same method of analysis is applied to the data for the membranes at 4 °C that are given in Table 1, the exchange rates derived are all close to zero, with the exception of native membranes, and the values derived for  $T_{1,b}^0$  are close to those given in Table 1. This is consistent with the approximation made above with regard to the lack of appreciable exchange at 4 °C. For native membranes at 4 °C, nonvanishing exchange rates of  $T_{1,f}^0\tau_b^{-1} = 0.3$  and  $0.1$  at pH 9.0 and 6.0, respectively, are calculated by this method. These are much lower, however, than those estimated for the native membranes at 25 °C.

## DISCUSSION

The aim of this work was to determine the dynamics of the lipid chains associated with the Na,K-ATPase in native membranes and to compare these with corresponding results from membranes that have been extensively trypsinized to remove the extramembranous part of the protein. Such an approach provides a sensitive test of the intactness of the native lipid–protein interface after trypsinization, which cleaves the peptide links between several of the transmembrane domains (6). By making measurements at low (4 °C) and high (25 °C) temperatures, and by comparing results at different pH values, for which the spin-labeled fatty acid displays different selectivities of interaction with the Na,K-ATPase (29), it was possible to make a consistent interpretation of the data in terms of both the chain dynamics of lipids in situ at the lipid–protein interface and the rate of exchange of these lipids with the bulk lipid pool in the fluid bilayer regions of the membrane. Because the rates of both of these processes lie close to the limits of dynamic sensitivity of conventional spin-label ESR (16, 19; see footnote 3), it was necessary to investigate the saturation properties of the spin-label ESR spectra, which are sensitive to the spin–lattice relaxation, the time scale of which lies in the microsecond regime (35).

*Local Rotational Chain Dynamics.* With the exception of the native membranes (for which there is a nonvanishing rate of exchange at 4 °C), the effective relaxation rates,

$1/(T_1T_2)_b^0$ , of the protein-associated lipid at 4 °C were of a similar magnitude for both ionized and protonated spin-labeled fatty acids (Table 1). This is despite the fact that the fractional populations are very different, reflecting the thermodynamic specificity for association with the ionized fatty acid, as compared to the protonated fatty acid (29). The protonated and ionized fatty acids therefore associate at similar sites at the lipid–protein interface but simply with different specificities.

The relaxation rates of the protein-associated lipids,  $1/(T_1T_2)_b^0$ , are considerably smaller than those of the fluid lipids,  $1/(T_1T_2)_L$ , at 4 °C (see Table 1). This reflects the restriction in rotational mobility of the lipid chains interacting directly with the intramembranous surface of the protein. On increasing the temperature to 25 °C, the effective relaxation rate of the protein-associated lipids  $1/(T_1T_2)_b^0$  increases—reflecting an increased mobility—but remains less than that of the fluid lipids, which hardly changes (Table 2). Recently, the effect of isotropic rotational motion on the saturation properties of spin labels, in progressive saturation experiments, has been investigated by theoretical spectral simulations (33). These latter results allow at least a qualitative interpretation of the relative relaxation rates of the protein-associated and fluid lipids and their temperature dependence (see Figure 4). These calculations (i.e., Figure 4) provide a theoretical calibration of the sensitivity of the intrinsic relaxation parameters to rotational dynamics that complements the relative scale established experimentally from comparison of the membrane and extracted lipid samples (cf. Results section, above). The effective relaxation rates are predicted to reach a maximum at an intermediate rotational correlation time on the order of 10 ns and to decrease on either side of this value, reaching a constant minimum value at either very long ( $\sim 1 \mu\text{s}$ ) or very short ( $\sim 0.1 \text{ ns}$ ) correlation times (33). Qualitatively, this type of biphasic behavior has been observed experimentally for the temperature dependence of the saturation parameters of spin-labeled lipids in sarcoplasmic reticulum membranes (16).

The increase in effective relaxation rate of the protein-associated lipids with increasing temperature indicates that their rotational correlation time lies on the slow-motion side of the maximum in the submicrosecond regime (see Figure 4), for which the relaxation rate is determined by spectral

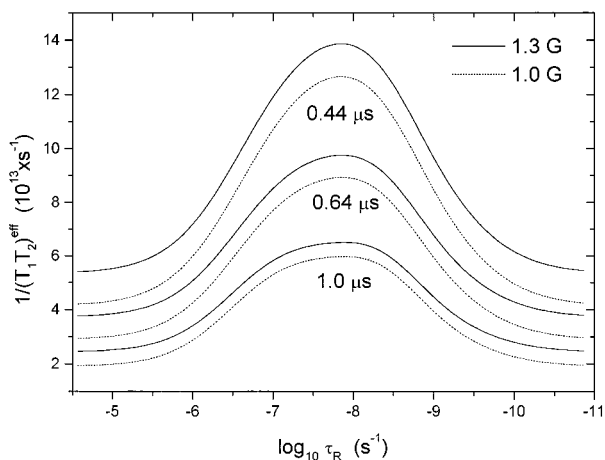


FIGURE 4: Dependence of the effective relaxation rate,  $1/(T_1T_2)^{\text{eff}}$ , deduced from theoretical simulations of progressive saturation experiments with a nitroxide spin label, on the isotropic rotational correlation time,  $\tau_R$ , of the spin label (33). Calculations are made for intrinsic Lorentzian line widths of  $\Delta H = 1.3$  G (solid lines) and  $\Delta H = 1.0$  G (dashed lines), and intrinsic spin–lattice relaxation times of  $T_1 = 0.44$ ,  $0.64$ , and  $1.0$   $\mu\text{s}$  (for each pair, from top to bottom).

diffusion (i.e., saturation transfer). This is confirmed by the fact that the relaxation rates are slower than those in dispersions of the extracted membrane lipids. The apparent lack of temperature dependence for the latter suggests that the relaxation rates are close to the maximum. Most probably, significant components of the motion switch from the slow motion regime to the motional narrowing nanosecond regime with increasing temperature, for the extracted lipids, although direct motional contributions to the intrinsic spin–lattice relaxation rate must also be included. Results for the extracted lipids are consistent with predictions for isotropic motion with an intrinsic line width of  $\Delta H = 1.3$  G and  $T_1 = 0.44$   $\mu\text{s}$  (see Figure 4). This value of  $T_1$  is comparable to those obtained previously by saturation methods for chains with this position of labeling in fluid membranes (33). The values of  $1/(T_1T_2)^{\text{eff}}$  for the motionally restricted lipids imply a longer  $T_1$  ( $\leq 1$   $\mu\text{s}$ ), however. These conclusions are qualitative because the rotational motion of the 14-SASL spin label is undoubtedly anisotropic.

Some difference is found in the intrinsic relaxation rates of the spin-labeled lipids,  $1/(T_1T_2)_b^0$ , between membranes trypsinized in the presence of  $\text{Rb}^+$  ions and those trypsinized in the presence of  $\text{Na}^+$  ions. For  $\text{Rb}$ -trypsinized membranes, the rates are somewhat slower than those found for the controls, but for  $\text{Na}$ -trypsinized membranes the rates are comparable to the controls (see Tables 1 and 2). The reason for this is not known with certainty, and the effect may not be very appreciable relative to the error limits. Membranes trypsinized in the presence of  $\text{Na}^+$  ions no longer retain the 19 kDa putative four-helix fragment that is associated with  $\text{Rb}$  occlusion capacity, which is preserved for membranes trypsinized in the presence of  $\text{Rb}^+$  ions (6). A modification of the dynamics of lipid–protein interaction, corresponding to a reduced chain mobility for  $\text{Rb}$ -trypsinized membranes, may be associated with this difference. In this connection it is interesting to note that attempts to identify residual minor fragments of the 19-kDa peptide on SDS gels, originating from the tryptic fragmentation of this peptide in the presence of  $\text{NaCl}$ , have so far not been successful. In addition, it also

should be noted that the temperature-dependent plasticity of the tryptic peptides seen with kidney enzyme (12, 13, 36) could be more marked with the shark enzyme used in the present experiments because of the greater mobility of the lipids in the shark membranes at a given temperature.

**Lipid Exchange Dynamics.** Ideally, one might expect that the results obtained from control membranes would be identical with those obtained from native membranes. However, this is not exactly the case (Tables 1 and 2). As noted in Results, lipid exchange takes place at a slow but significant rate in native membranes, even at 4  $^{\circ}\text{C}$  ( $\tau_b \sim 2, 7 \times 10^5$   $\text{s}^{-1}$  at pH 6, 9, respectively), and the exchange rates estimated at 25  $^{\circ}\text{C}$  are higher for native than for control membranes (see Table 2). Changes must be taking place in the membrane during the incubation period to which control membranes are subjected that account for this difference. Previously, temperature- and time-dependent changes, in the direction of decreased mobility, have been detected in the saturation transfer ESR spectra of spin-labeled membranous  $\text{Na,K-ATPase}$ , on incubation at temperatures above 20  $^{\circ}\text{C}$  (31). The origin of these changes is not known with certainty, but the decreased lipid exchange rates in control membranes are clearly linked with these changes in microsecond motions of the protein. This difference between native and control membranes therefore illustrates the sensitivity of the lipid spin-label relaxation parameters to changes in the protein dynamics. In addition, the shark enzyme progressively loses activity on incubation at elevated temperatures that are well below that of thermal denaturation, correlating with the alteration in membrane dynamics (37). [Thermal unfolding, and even hydrophobic mismatch, results in more dramatic changes in lipid–protein interactions than simply an alteration in exchange dynamics (38).] For the purposes of the present work, incubated membranes are therefore the appropriate controls for comparison with trypsinized membranes.

The results of Table 2 indicate that the exchange of lipids at the intramembranous surface of the  $\text{Na,K-ATPase}$  takes place continuously with those in the bulk lipid regions of the membrane, on the time scale of the spin–lattice relaxation of the spin-labeled lipids, i.e., in the microsecond time regime. This is true both for control membranes and for trypsinized membranes.<sup>4</sup> The lipid exchange rates in the trypsinized membranes tend to be slower than those for the corresponding control membranes (see Table 2). This change is in the same direction as that found between native and control membranes, although the differences in rates are considerably smaller than for the latter case and lie within the maximum error limits. Possibly, this reflects the same time- and temperature-dependent change discussed previously, which becomes somewhat accelerated in the case of the trypsinized membranes as compared with the controls. (Note that these differences between the saturation parameters for the various membrane preparations appear consistently within the matched series and therefore the errors of the corresponding mean values are to some extent correlated.)

<sup>4</sup> Only in one case in Table 2 (i.e.,  $\text{Na}$ -trypsin at pH 9.0) does the lower error limit of the exchange rate apparently reach zero (to within the quoted precision). However, this rate must still be appreciable, because the lower extreme value at pH 6.0 is nonzero, and that at pH 9.0 is related to this by the ratio of relative association constants ( $=2-2.5$ ) according to eq 6.

Exchange rates for membranes trypsinized in the presence of Na<sup>+</sup> ions are similar to those for membranes trypsinized in the presence of Rb<sup>+</sup> ions, for both ionized and protonated fatty acids. Differences associated with the intactness of the 19 kDa fragment are therefore not reflected strongly in the lipid exchange rates.

Differences in exchange rate between the ionized and protonated fatty acid, in the direction of faster exchange for the latter, are observed in all cases (see Table 2). This directly reflects the specificity of the ionized relative to the protonated species for lipid-protein interaction of fatty acids with the Na,K-ATPase (cf. ref 34). The ratio of association constants can be deduced from the lipid off-rates  $T_{1\rho}^0\tau_b^{-1}$  by combining eq 5 with the expression for equilibrium lipid-protein exchange association (see ref 39):

$$\frac{\tau_b^{-1}(\text{LH})}{\tau_b^{-1}(\text{L}^-)} = \frac{f_{\text{L}^-}(1 - f_{\text{LH}})}{f_{\text{LH}}(1 - f_{\text{L}^-})} = \frac{K_r(\text{L}^-)}{K_r(\text{LH})} \quad (6)$$

where L<sup>-</sup> and LH refer to the ionized and protonated fatty acid, respectively, and  $K_r$  is the relative association constant. This yields values in the region of  $K_r(\text{L}^-)/K_r(\text{LH}) = 2-2.5$ , for ionized relative to protonated fatty acid, in agreement with previous equilibrium thermodynamic studies (14). (Note that the errors in the derived quantities for a given preparation are strictly correlated at the two pH values—i.e., upper suffixes must be compared consistently with upper suffixes, etc.—preserving the ratio of exchange rates.) It therefore may be concluded that the lipid chains directly contacting the Na,K-ATPase have temperature-dependent, submicrosecond segmental motions and that these first-shell lipid molecules exchange with the bulk membrane lipids on the microsecond time scale. These essential features of the dynamics of the lipid-protein interaction with the Na,K-ATPase are largely preserved on removal of the extramembranous portions of the protein by extensive trypsinization.

## ACKNOWLEDGMENT

We thank Frau B. Angerstein for preparation of spin-labeled lipids and Ms. Birthe Bjerring Jensen and Ms. Angielina Damgaard of the University of Aarhus for skillful technical assistance.

## REFERENCES

- Esmann, M., Watts, A., and Marsh, D. (1985) *Biochemistry* 24, 1386–1393.
- Marsh, D. (1993) in *New Comprehensive Biochemistry, Vol. 25, Protein-Lipid Interactions*. (Watts, A., Ed.) pp 41–66, Elsevier, Amsterdam.
- Marsh, D. (1997) *Eur. Biophys. J.* 26, 203–208.
- Karlish, S. J. D., Goldshleger, R., and Stein, W. D. (1990) *Proc. Natl. Acad. Sci. U.S.A.* 87, 4566–4570.
- Ning, G., Maunsbach, A. B., and Esmann, M. (1993) *FEBS Lett.* 330, 19–22.
- Esmann, M., Karlish, S. J. D., Sottrup-Jensen, L., and Marsh, D. (1994) *Biochemistry* 33, 8044–8050.
- Karlish, S. J. D. (1997) *Ann. N.Y. Acad. Sci.* 834, 30–44.
- Fambrough, D. M., Lemas, M. V., Hamrick, M., Emerick, M., Renaud, K. J., Inman, E. M., Hwang, B. and Takeyasu, K. (1994) *Am. J. Physiol.* 266, 579–589.
- Lutsenko, S., and Kaplan, J. H. (1993) *Biochemistry* 32, 6737–6743.
- Ivanov, A., Askari, A., and Modyanov, N. N. (1997) *FEBS Lett.* 420, 107–111.
- Or, E., Goldshleger, R., Shainskaya, A., and Karlish, S. J. D. (1998) *Biochemistry* 37, 8197–8207.
- Lutsenko, S., Anderko, R. and Kaplan, J. H. (1995) *Proc. Natl. Acad. Sci. U.S.A.* 92, 7936–7940.
- Shainskaya, A., Nesaty, V., and Karlish, S. J. D. (1998) *J. Biol. Chem.* 273, 7311–7319.
- Arora, A., Esmann, M., and Marsh, D. (1998) *Biochim. Biophys. Acta* 1371, 163–167.
- Marsh, D., Páli, T., and Horváth, L. I. (1998) in *Biological Magnetic Resonance, Vol. 14, Spin Labeling. The Next Millennium* (Berliner, L. J., Ed.) Chapter 2, pp 23–82, Plenum Press, New York.
- Squier, T. C., and Thomas, D. D. (1989) *Biophys. J.* 56, 735–748.
- Horváth, L. I., Brophy, P. J., and Marsh, D. (1993) *Biophys. J.* 64, 622–631.
- Marsh, D., and Horváth, L. I. (1998) *Biochim. Biophys. Acta* 1376, 267–296.
- Horváth, L. I., Brophy, P. J., and Marsh, D. (1988) *Biochemistry* 27, 46–52.
- Skou, J. C., and Esmann, M. (1979) *Biochim. Biophys. Acta* 567, 436–444.
- Esmann, M. (1988) *Methods Enzymol.* 156, 105–155.
- Bligh, E. G., and Dyer, W. J. (1959) *Can. J. Biochem. Physiol.* 37, 911–917.
- Esmann, M., and Sottrup-Jensen, L. (1992) *Biochim. Biophys. Acta* 1112, 247–252.
- Marsh, D., and Watts, A. (1982) in *Lipid-Protein Interactions, Vol. 2* (Jost, P. C., and Griffith, O. H., Eds.) pp 53–126, Wiley-Interscience, New York.
- Marsh, D. (1982) in *Techniques in Lipid and Membrane Biochemistry, Vol. (Metcalf, J. C., and Hesketh, T. R., Eds.) Vol. B4/II*, pp B426/1–44, Elsevier, Amsterdam.
- Fajer, P., and Marsh, D. (1982) *J. Magn. Reson.* 49, 212–224.
- Snel, M. M. E., and Marsh, D. (1993) *Biochim. Biophys. Acta* 1150, 155–161.
- Páli, T., Horváth, L. I., and Marsh, D. (1993) *J. Magn. Reson. A101*, 215–219.
- Esmann, M., and Marsh, D. (1985) *Biochemistry* 24, 3572–3578.
- Esmann, M., Hideg, K., and Marsh, D. (1988) *Biochemistry* 27, 3913–3917.
- Esmann, M., Horváth, L. I., and Marsh, D. (1987) *Biochemistry* 26, 8675–8683.
- Esmann, M., and Marsh, D. (1992) *Proc. Natl. Acad. Sci. U.S.A.* 89, 7606–7609.
- Livshits, V. A., Páli, T., and Marsh, D. (1998) *J. Magn. Reson.* 133, 79–91.
- Horváth, L. I., Brophy, P. J., and Marsh, D. (1988) *Biochemistry* 27, 5296–5304.
- Marsh, D. (1993) *Chem. Soc. Rev.* 22, 329–335.
- Liu, L., and Askari, A. (1997) *J. Biol. Chem.* 272, 14380–14386.
- Heimburg, T., Esmann, M., and Marsh, D. (1997) *J. Biol. Chem.* 272, 25686–25692.
- Ryba, N. J. P., and Marsh, D. (1992) *Biochemistry* 31, 7511–7518.
- Marsh, D., and Horváth, L. I. (1989) in *Advanced EPR. Applications in Biology and Biochemistry* (Hoff, A. J., Ed.) pp 707–752, Elsevier, Amsterdam.